Emergence of intraband transitions in colloidal nanocrystals

Amardeep Jagtap, Clément Livache, Bertille Martinez, Junling Qu, Audrey Chu, Charlie Gréboval, Nicolas Goubet, Emmanuel Lhuillier

Emergence of intraband transitions in colloidal nanocrystals [Invited]

AMARDEEP JAGTAP, CLÉMENT LIVACHE, BERTILLE MARTINEZ, JUNLING QU, AUDREY CHU, CHARLIE GRÉBOVAL, NICOLAS GOUBET, AND EMMANUEL LHUILLIER*

Sorbonne Université, UPMC Univ. Paris 06, CNRS-UMR 7588, Institut des NanoSciences de Paris, 4 place Jussieu, 75005 Paris, France
**el@insp.upmc.fr*

Abstract: The chemistry of nanocrystals enables the receipt of semiconductor nanoparticles with tunable optical properties. So far most scientific efforts have been focused on wide band gap materials to achieve a bright luminescence and a higher solar power conversion efficiency. Their properties in the infrared range of wavelengths are interesting as well. Two strategies can be used to achieve mid-infrared (mid-IR) transition, either interband transition in narrow band gap material or intraband transition in doped material. In this review, we discuss recent progress to achieve stable doped nanocrystals. We focus on mercury chalcogenide compounds since they are so far the only materials that combine mid-IR absorption with photoconductive properties in this range of energies. We discuss the origin of the doping and its tunability as well as how the doping impacts the optical, transport, and photodetection properties. Finally, we discuss Hg-free alternative materials, and present mid-IR transitions.

OCIS codes: (040.3060) Infrared; (040.5160) photodetectors; (250.5590) Quantum-well, -wire and -dot devices.

References and links

1. L. Esaki, "Long journey into tunneling," Rev. Mod. Phys. **46**(2), 237–244 (1974).
2. L. Esaki and R. Tsu, "Superlattice and negative differential conductivity in semiconductors," IBM J. Res. Develop. **14**(1), 61–65 (1970).
3. L. L. Chang, L. Esaki, and R. Tsu, "Resonant tunneling in semiconductor double barriers," Appl. Phys. Lett. **24**(12), 593–595 (1974).
4. L. Esaki and L. L. Chang, "New Transport Phenomenon in a Semiconductor "Superlattice,"," Phys. Rev. Lett. **33**(8), 495–498 (1974).
5. A. Rogalski, J. Antoszewski, and L. Faraone, "Third-generation infrared photodetector arrays," J. Appl. Phys. **105**(9), 091101 (2009).
6. B. F. Levine, "Quantum-well infrared photodetectors," J. Appl. Phys. **74**(8), R1–R81 (1993).
7. H. Schneider and H. C. Liu, "Quantum well infrared photodetectors," Physics and applications (Springer, Heidelberg, 2006).
8. J. Faist, F. Capasso, D. L. Sivco, C. Sirtori, A. L. Hutchinson, and A. Y. Cho, "Quantum cascade laser," Science **264**(5158), 553–556 (1994).
9. J. Phillips, K. Kamath, and P. Bhattacharya, "Far-infrared photoconductivity in self-organized InAs quantum dots," Appl. Phys. Lett. **72**(16), 2020–2022 (1998).
10. P. Martyniuk and A. Rogalski, "Quantum-dot infrared photodetectors: Status and outlook," Prog. Quantum Electron. **32**(3-4), 89–120 (2008).
11. M. A. Hines and P. Guyot-Sionnest, "Synthesis and characterization of strongly luminescing ZnS-capped CdSe nanocrystals," J. Phys. Chem. **100**(2), 468–471 (1996).
12. E. Izquierdo, A. Robin, S. Keuleyan, N. Lequeux, E. Lhuillier, and S. Ithurria, "Strongly confined HgTe 2D nanoplatelets as narrow near infrared emitter," J. Am. Chem. Soc. **138**(33), 10496–10501 (2016).
13. C. Livache, E. Izquierdo, B. Martinez, M. Dufour, D. Pierucci, S. Keuleyan, H. Cruguel, L. Becerra, J.-L. Fave, H. Aubin, A. Ouerghi, E. Lacaze, M. G. Silly, B. Dubertret, S. Ithurria, and E. Lhuillier, "Charge dynamics and optolectronic properties in HgTe colloidal quantum wells," Nano Lett. **17**(7), 4067–4074 (2017).
14. M. Nasilowski, B. Mahler, E. Lhuillier, S. Ithurria, and B. Dubertret, "Two-Dimensional Colloidal nanocrystals," Chem. Rev. **116**(18), 10934–10982 (2016).
15. M. A. Boles, M. Engel, and D. V. Talapin, "Self-assembly of colloidal nanocrystals: from intricate structures to functional materials," Chem. Rev. **116**(18), 11220–11289 (2016).

16. M. A. Hines and G. D. Scholes, “Colloidal PbS nanocrystals with size-tunable near-infrared emission: observation of post-synthesis self-narrowing of the particle size distribution,” Adv. Mater. **15**(21), 1844–1849 (2003).
17. O. E. Semonin, J. M. Luther, S. Choi, H. Y. Chen, J. Gao, A. J. Nozik, and M. C. Beard, “Peak external photocurrent quantum efficiency exceeding 100% via MEG in a quantum dot solar cell,” Science **334**(6062), 1530–1533 (2011).
18. M. Böberl, M. V. Kovalenko, S. Gamerith, E. List, and W. Heiss, “Inkjet-printed nanocrystal photodetectors operating up to 3 μm wavelengths,” Adv. Mater. **19**(21), 3574–3578 (2007).
19. S. Keuleyan, E. Lhuillier, V. Brajuskovic, and P. Guyot-Sionnest, “Mid-infrared HgTe colloidal quantum dot photodetectors,” Nat. Photonics **5**(8), 489–493 (2011).
20. P. Guyot-Sionnest, M. Shim, C. Matranga, and M. Hines, “Intraband relaxation in CdSe quantum dots,” Phys. Rev. B **60**(4), 2181–2184 (1999).
21. C. Wang, M. Shim, and P. Guyot-Sionnest, “Electrochromic nanocrystal quantum dots,” Science **291**(5512), 2390–2392 (2001).
22. A. Sahu, M. S. Kang, A. Kompch, C. Notthoff, A. W. Wills, D. Deng, M. Winterer, C. D. Frisbie, and D. J. Norris, “Electronic impurity doping in CdSe nanocrystals,” Nano Lett. **12**(5), 2587–2594 (2012).
23. D. J. Norris, A. L. Efros, and S. C. Erwin, “Doped nanocrystals,” Science **319**(5871), 1776–1779 (2008).
24. Z. Deng, K. S. Jeong, and P. Guyot-Sionnest, “Colloidal quantum dots intraband photodetectors,” ACS Nano **8**(11), 11707–11714 (2014).
25. E. Lhuillier, M. Scarafagio, P. Hease, B. Nadal, H. Aubin, X. Z. Xu, N. Lequeux, G. Patriarche, S. Ithurria, and B. Dubertret, “Infrared photo-detection based on colloidal quantum-dot films with high mobility and optical absorption up to the THz,” Nano Lett. **16**(2), 1282–1286 (2016).
26. S. Keuleyan, E. Lhuillier, and P. Guyot-Sionnest, “Synthesis of Colloidal HgTe Quantum Dots for Narrow Mid-IR Emission and Detection,” J. Am. Chem. Soc. **133**(41), 16422–16424 (2011).
27. S. E. Keuleyan, P. Guyot-Sionnest, C. Delerue, and G. Allan, “Mercury telluride colloidal quantum dots: Electronic structure, size-dependent spectra, and photocurrent detection up to 12 μm,” ACS Nano **8**(8), 8676–8682 (2014).
28. K. S. Jeong, Z. Deng, S. Keuleyan, H. Liu, and P. Guyot-Sionnest, “Air-stable n-doped colloidal HgS quantum dots,” J. Phys. Chem. Lett. **5**(7), 1139–1143 (2014).
29. J. Kim, B. Yoon, J. Kim, Y. Choi, Y. W. Kwon, S. K. Park, and K. S. Jeong, “High electron mobility of β-HgS colloidal quantum dots with doubly occupied quantum states,” RSC Advances **7**(61), 38166–38170 (2017).
30. J. Jeong, B. Yoon, Y. W. Kwon, D. Choi, and K. S. Jeong, “Singly and Doubly Occupied Higher Quantum States in Nanocrystals,” Nano Lett. **17**(2), 1187–1193 (2017).
31. N. Goubet, A. Jagtap, C. Livache, B. Martinez, H. Portales, X. Zhen Xu, R.P.S.M. Lobo, B. Dubertret, and E. Lhuillier, “Terahertz HgTe nanocrystals: beyond confinement,” submitted (2017).
32. G. Shen, M. Chen, and P. Guyot-Sionnest, “Synthesis of Nonaggregating HgTe Colloidal Quantum Dots and the Emergence of Air-Stable n-Doping,” J. Phys. Chem. Lett. **8**(10), 2224–2228 (2017).
33. B. Martinez, C. Livache, L. D. Notemgnou Mouafo, N. Goubet, S. Keuleyan, H. Cruguel, S. Ithurria, H. Aubin, A. Ouerghi, B. Doudin, E. Lacaze, B. Dubertret, M. G. Silly, R. P. S. M. Lobo, J. F. Dayen, and E. Lhuillier, “HgSe self-doped nanocrystals as a platform to investigate the effects of vanishing confinement,” ACS Appl. Mater. Interfaces **9**(41), 36173–36180 (2017).
34. E. Lhuillier, S. Keuleyan, and P. Guyot-Sionnest, “Optical properties of HgTe colloidal quantum dots,” Nanotechnology **23**(17), 175705 (2012).
35. A. Robin, C. Livache, S. Ithurria, E. Lacaze, B. Dubertret, and E. Lhuillier, “Surface Control of Doping in Self-Doped Nanocrystals,” ACS Appl. Mater. Interfaces **8**(40), 27122–27128 (2016).
36. H. Liu, C. K. Brozek, S. Sun, D. B. Lingerfelt, D. R. Gamelin, and X. Li, “A Hybrid Quantum-Classical Model of Electrostatics in Multiply Charged Quantum Dots,” J. Phys. Chem. C **121**(46), 26086–26095 (2017).
37. M. Chen and P. Guyot-Sionnest, “Reversible Electrochemistry of Mercury Chalcogenide Colloidal Quantum Dot Films,” ACS Nano **11**(4), 4165–4173 (2017).
38. L. K. Sagar, W. Walravens, J. Maes, P. Geiregat, and Z. Hens, “HgSe/CdE (E = S, Se) Core/Shell Nanocrystals by Colloidal Atomic Layer Deposition,” J. Phys. Chem. C **121**(25), 13816–13822 (2017).
39. Z. Deng and P. Guyot-Sionnest, “Intraband Luminescence from HgSe/CdS Core/Shell Quantum Dots,” ACS Nano **10**(2), 2121–2127 (2016).
40. G. Shen and P. Guyot-Sionnest, “HgS and HgS/CdS Colloidal Quantum Dots with Infrared Intraband Transitions and Emergence of a Surface Plasmon,” J. Phys. Chem. C **120**(21), 11744–11753 (2016).
41. V. I. Klimov, A. A. Mikhailovsky, D. W. McBranch, C. A. Leatherdale, and M. G. Bawendi, “Mechanisms for intraband energy relaxation in semiconductor quantum dots: The role of electron-hole interactions,” Phys. Rev. B **61**(20), R13349(R) (2000).
42. P. Sippel, W. Albrecht, J. C. van der Bok, R. J. A. Van Dijk-Moes, T. Hannappel, R. Eichberger, and D. Vanmaekelbergh, “Femtosecond Cooling of Hot Electrons in CdSe Quantum-Well Platelets,” Nano Lett. **15**(4), 2409–2416 (2015).
43. E. Lhuillier, S. Ithurria, A. Descamps-Mandine, T. Douillard, R. Castaing, X. Z. Xu, P.-L. Taberna, P. Simon, H. Aubin, and B. Dubertret, “Investigating the n and p type electrolytic charging of colloidal nanoplatelets,” J. Phys. Chem. C **119**(38), 21795–21799 (2015).

44. E. Lhuillier, A. Robin, S. Ithurria, H. Aubin, and B. Dubertret, “Electrolyte-gated colloidal nanoplatelets-based phototransistor and its use for bicolor detection,” Nano Lett. **14**(5), 2715–2719 (2014).
45. H. Wang, E. Lhuillier, Q. Yu, A. Zimmers, B. Dubertret, C. Ulysse, and H. Aubin, “Transport in a Single Self-Doped Nanocrystal,” ACS Nano **11**(2), 1222–1229 (2017).
46. A. L. Roest, J. J. Kelly, D. Vanmaekelbergh, and E. A. Meulenkamp, “Staircase in the Electron Mobility of a ZnO Quantum Dot Assembly due to Shell Filling,” Phys. Rev. Lett. **89**(3), 036801 (2002).
47. X. Tang, G. F. Wu, and K. W. C. Lai, “Plasmon resonance enhanced colloidal HgSe quantum dot filterless narrowband photodetectors for mid-wave infrared,” J. Mater. Chem. C Mater. Opt. Electron. Devices **5**(2), 362–369 (2017).
48. E. Lhuillier and P. Guyot Sionnest, “Recent Progresses in Mid Infrared Nanocrystal based Optoelectronics,” IEEE J. Sel. Top. Quantum Electron. **23**(5), 1–8 (2017).
49. A. Sahu, A. Khare, D. D. Deng, and D. J. Norris, “Quantum confinement in silver selenide semiconductor nanocrystals,” Chem. Commun. (Camb.) **48**(44), 5458–5460 (2012).
50. A. Sahu, L. Qi, M. S. Kang, D. Deng, and D. J. Norris, “Facile synthesis of silver chalcogenide (Ag2E; E=Se, S, Te) semiconductor nanocrystals,” J. Am. Chem. Soc. **133**(17), 6509–6512 (2011).
51. C. Delerue, “Minimum Line Width of Surface Plasmon Resonance in Doped ZnO Nanocrystals,” Nano Lett. **17**(12), 7599–7605 (2017).
52. E. Della Gaspera, M. Bersani, M. Cittadini, M. Guglielmi, D. Pagani, R. Noriega, S. Mehra, A. Salleo, and A. Martucci, “Low-Temperature Processed Ga-doped ZnO Coatings from Colloidal Inks,” J. Am. Chem. Soc. **135**(9), 3439–3448 (2013).
53. S. Ghosh, M. Saha, and S. K. De, “Tunable surface plasmon resonance and enhanced electrical conductivity of In doped ZnO colloidal nanocrystals,” Nanoscale **6**(12), 7039–7051 (2014).
54. R. Buonsanti, A. Llordes, S. Aloni, B. A. Helms, and D. J. Milliron, “Tunable Infrared Absorption and Visible Transparency of Colloidal Aluminum-Doped Zinc Oxide Nanocrystals,” Nano Lett. **11**(11), 4706–4710 (2011).
55. M. Shim and P. Guyot-Sionnest, “Organic-Capped ZnO Nanocrystals: Synthesis and n-Type Character,” J. Am. Chem. Soc. **123**(47), 11651–11654 (2001).
56. M. Kanehara, H. Koike, T. Yoshinaga, and T. Teranishi, “Indium Tin Oxide Nanoparticles with Compositionally Tunable Surface Plasmon Resonance Frequencies in the Near-IR Region,” J. Am. Chem. Soc. **131**(49), 17736–17737 (2009).
57. E. L. Runnerstrom, A. Bergerud, A. Agrawal, R. W. Johns, C. J. Dahlman, A. Singh, S. M. Selbach, and D. J. Milliron, “Defect Engineering in Plasmonic Metal Oxide Nanocrystals,” Nano Lett. **16**(5), 3390–3398 (2016).
58. A. M. Schimpf, S. D. Lounis, E. L. Runnerstrom, D. J. Milliron, and D. R. Gamelin, “Redox Chemistries and Plasmon Energies of Photodoped In2O3 and Sn-Doped In2O3 (ITO) Nanocrystals,” J. Am. Chem. Soc. **137**(1), 518–524 (2015).
59. B. Tandon, A. Yadav, D. Khurana, P. Reddy, P. K. Santra, and A. Nag, “Size-Induced Enhancement of Carrier Density, LSPR Quality Factor,and Carrier Mobility in Cr–Sn Doped In2O3 Nanocrystals,” Chem. Mater. **29**(21), 9360–9368 (2017).
60. T. Chen, K. V. Reich, N. J. Kramer, H. Fu, U. R. Kortshagen, and B. I. Shklovskii, “Metal-insulator transition in films of doped semiconductor nanocrystals,” Nat. Mater. **15**(3), 299–303 (2016).
61. R. Gresback, N. J. Kramer, Y. Ding, T. Chen, U. R. Kortshagen, and T. Nozaki, “Controlled Doping of Silicon Nanocrystals Investigated By Solution-Processed Field Effect Transistors,” ACS Nano **8**(6), 5650–5656 (2014).
62. H. Zhang, R. Zhang, K. S. Schramke, N. M. Bedford, K. Hunter, U. R. Kortshagen, and P. Nordlander, “Doped Silicon Nanocrystal Plasmonics,” ACS Photonics **4**(4), 963–970 (2017).
63. D. J. Rowe, J. S. Jeong, K. A. Mkhoyan, and U. R. Kortshagen, “Phosphorus-Doped Silicon Nanocrystals exhibiting Mid-Infrared Localized Surface Plasmon Resonance,” Nano Lett. **13**(3), 1317–1322 (2013).

1. Introduction

Infrared (IR) technologies remain driven by epitaxially grown materials made of III-V and II-VI semiconductors. There are two types of approaches for engineering materials with low energy transition, which is required for IR photon absorption. The first method relies on interband transition in narrow band gap material (InGaAs in the near infrared or HgCdTe in the mid-IR). In this case, the wavelength tunability is based on metallurgy skills to tune finely the ratio of two binary semiconductors mixed in a ternary alloy. A completely different approach relies on intersubband transition in heterostructures made of wide band gap semiconductors (mostly III-V compounds such as GaAs/AlGaAs). By doping such heterostructures, intersubband transitions (usually in the conduction band) can be used to reach narrow energy transition in the IR range. The growth of such heterostructures strongly relies on the development of epitaxial methods in the late 70’s and 80’s and has reached a high level of success [1–4] with the development of infrared detectors [5] based on multiquantum well structures [6] (also called QWIP for Quantum well infrared Photodetector [7]) and laser sources such as the quantum cascade laser [8].

In this review, we will focus on the photodetection side. The QWIP technology is based on a weakly-coupled series of quantum wells, with typically two levels: one ground state and one excited state, generally resonant with the barrier. The QWIP benefits from the maturity and high homogeneity of III-V materials, which allows the production of large scale matrices. Also, the high quality of III-V materials leads to a low level of noise with no 1/f component. On the other hand, QWIPs suffer from a high dark current, which is inherent to the doping needed to obtain intersubband transition and leads to low cryogenic operating temperature. A second key drawback results from the absorption selection rules of quantum well, which make the QWIPs not absorbing the normally incident light. As a result, a grating must be etched at the surface of the pixel to scatter back the light and obtain a reasonable level of absorption. In the 90's, solid-state quantum dots [9] based infrared photodetector [10] (QDIPs) has been proposed as a path to improve the performance of QWIPs. QDIPs benefit, in principle, from two key improvements. They have a discrete electronic spectrum and thus the coupling to phonon should be reduced, which raises the (unfulfilled) hope of increasing the operating temperature. Compared to quantum well based structures, QDIPs should also have removed the need for a diffraction grating since different selection rules apply for 0D structure. However, Stransky-Krastanov grown quantum dots remain quite flat and with a weak density ($< 10^{12}$ cm^{-2}), which overall leads to a weak absorption of the light in normal incidence.

In addition to performances, there is also requirement for developing the low-cost detectors, with in mind the need to expand applications of IR detectors, which are currently limited to defense and astronomy applications. New needs, such as assistance to night driving are emerging as affordable self-driven car will require low cost focal plane array (<1000 $). Such cost disruption is unlikely to result from historical technologies and intrinsically new low-cost technologies must be explored. Among potential candidates, colloidal quantum dots (CQDs) raise great hopes. Their synthesis started in the 90's with the development of new synthetic procedures leading to highly monodisperse nanocrystal solutions. The growth methods have rapidly expanded to reach a high level of maturity, which includes the synthesis of colloidal heterostructures [11], control of shape [12,13] and dimensionality [14], as well as self-assembly of nanoparticles [15]. The synthesis of CQDs was initially focused on II-VI wide band gap semiconductors but III-V compounds have also been investigated to obtain heavy metal-free nanoparticles. CQDs are one of the examples of successful nanotechnologies, which have met a mass market application. For the last three years, they have been used as narrow green and red sources in the last generation of LCD displays with enhanced gamut. Narrow band gap materials, in particular PbS [16] and CIGS (CuGaInS(e) and derivatives) have also attracted interest starting from the 2000's for the design of solar cells. Interest for CQD-based solar cells was mainly motivated by the low threshold of multi-exciton generation [17]. It is only recently that the optical properties of CQDs have reached the mid-IR range with absorption features above 3 μm [18,19]. Most of the early results have been based on interband transitions in narrow band gap semiconductors and semimetals. Intraband transitions were also observed in CQDs, but only under optical [20] or electrochemical pumping [21]. Significant synthetic improvements [22,23] have been obtained over the recent years for the control of doping in CQDs, which enabled the observation of air-stable intraband transitions and their use for photodetection [24]. In this review, we discuss recent progresses relative to the observation and use of mid-IR intraband transitions. The first section of this review gives a brief introduction to colloidal nanocrystals and their properties. The second part is focused on mercury chalcogenides, which are by far the most investigated materials for IR detection based on CQDs. We mention the material synthesis improvements, which have made it possible to push the absorption up to the THz range. Transport and photodetection performances are also discussed. The third section is dedicated to Hg free CQD materials, which also present some intraband or plasmonic feature

in the mid IR. Finally, we draw some necessary ways of improvement to make this new design path for CQD-based devices effective.

2. Colloidal nanocrystals

CQDs are semiconductor nanoparticles with a size close to the materials Bohr radius in order to induce quantum confinement effect, see Fig. 1(a). They differ from self-assembled quantum dots grown by Stransky-Krastanov approach due to their electrical, mechanical, optical and acoustical mismatches with the environment. The crystalline growth occurs in solution without the need of a substrate, see electron microscopy image in Fig. 1(b). Another striking difference is the presence of ligands all around the CQD, see Fig. 1(c). Ligands are organic molecules made of an organic function, which sticks to the CQD surface and an alkane chain with typically 12 to 18 carbons. Ligands (*i*) ensure the preservation of the nm size of the particle by making the surface poorly available to chemical precursor and consequently limiting the crystal growth, (*ii*) make the nanoparticles colloidally stable in solution and (iii) finally participate to the surface electronic passivation by hybridizing the dangling bonds. Interests for the CQDs result from their bright luminescence, see Fig. 1(d), which is tunable all over the visible in the case of wide band gap material such as CdSe, see Fig. 1(e). Excellent monodispersity of the CQDs in solution ensures that the sparse density of state leads to atom like spectrum even for ensemble measurements, see Fig. 1(d).

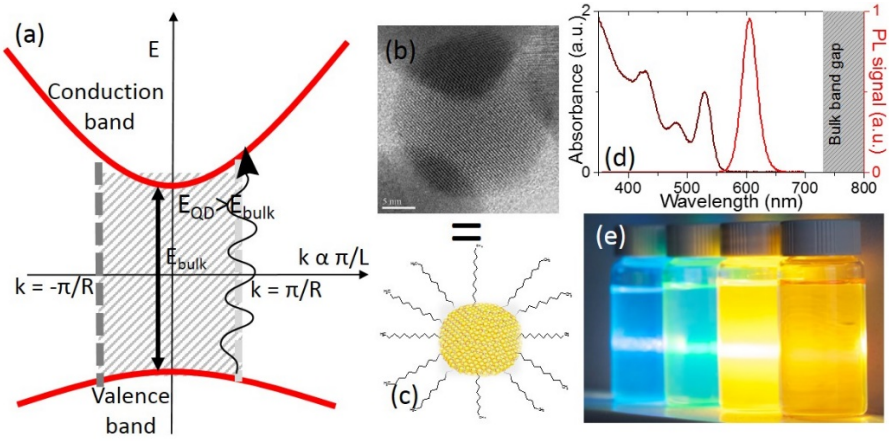

Fig. 1. (a) Band diagram of a semiconductor, showing how the band edge energy is enhanced in the presence of confinement. (b) TEM image of a HgSe nanocrystal and (c) its schematic highlighting the presence of ligands. (d) Absorption and photoluminescnce spectra of a CdSe/CdS nanocrystal solution. (e) Image of a solution of CdSe based nanocrystals with various levels of confinement.

3. Narrow band gap nanocrystals

II-VI semiconductors are by far the most investigated semiconductor nanocrystals. While cadmium based materials present excellent optical features in the visible range of wavelengths, mercury chalcogenides present absorption in the IR range. As bulk material, HgTe and HgSe are semimetals (i.e. their band gap is null), see the band structure in Fig. 2(a). As processed under a nanoparticle form, a band gap opens, which purely results from confinement. Over the last few years, a race has emerged to push further in the IR the absorption of CQDs, starting from the near IR range and now reaching the THz range [25]. Materials based on interband transition in HgTe CQDs, with optical features in the Mid Wave Infrared Range (MWIR: 3-5 µm) have been first reported by Keuleyan et al [18,26] (see Fig. 2(c)) and the same team has reached the Long Wave Infrared Range (LWIR: 8-12 µm) few years later [27], see Fig. 2(d). Parallel to this work, self-doped nanocrystals of HgS [28,29],

HgSe [24,25,30] and HgTe [31,32] started to be synthesized. Their absorption spectrum typically presents two contributions: one at high energy (visible and near IR) attributed to interband transition and one in the mid infrared due to an intraband transition, see Fig. 2(b). While initially this intraband transition was in the MWIR, our group rapidly expanded the range of available sizes to push this feature in the LWIR [25] and even further [33], see Fig. 2(e-f). By growing large size CQDs, it is now possible to obtain optical features which even overlap with the phonon absorption [31] (125 cm^{-1} in HgTe), see Fig. 2(f).

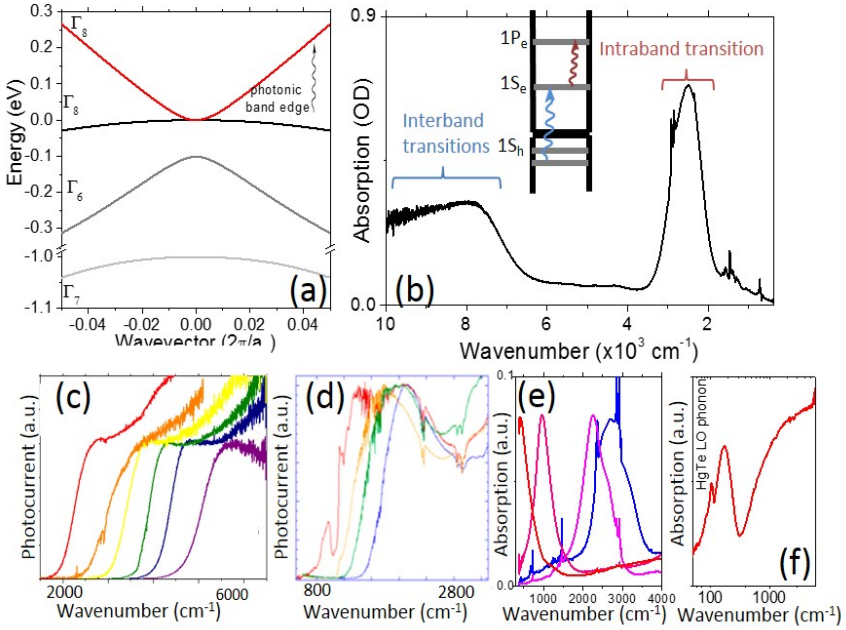

Fig. 2. (a) Band diagram of HgTe, adapted from [34]. (b) Infrared absorption spectrum of a HgSe nanocrystal film. (c) Photocurrent spectra of HgTe CQDs with absorption in the MWIR, adapted with permission from [25], Copyright (2016) American Chemical Society. (d) Photocurrent spectra of HgTe CQDs with absorption in the LWIR, adapted with permission from [27], Copyright (2016) American Chemical Society. € Absorption spectra of HgSe CQDs with optical features in the Far IR, adapted with permission from [33], Copyright (2016) American Chemical Society. (f) Absorption spectra of HgTe CQDs with absorption up to the THz range, adapted from [32].

4. Intraband transition in nanocrystals

Doping is a critical aspect for obtaining an intraband absorption. HgS [28,29], HgSe [24,30,25] and HgTe [32] have been described as self-doped materials since no extrinsic impurities are introduced during the growth. However, the presence of free electrons requires some compensating charges to keep the material neutral. Mercury chalcogenides have been found to be cation-rich compounds from energy dispersive X-ray spectroscopy measurements [30,35]. In other words, HgSe CQDs are made of an intrinsic material with an excess of Hg^{2+} on the surface. Depending on the ligands, this excess of positive charges might be partly screened, but the density of ligands will remain lower than the surface density of cations. This causes the bands to bend downwards and favors the injection of free electrons [36]. A more electrochemical way to understand this self-doping process is the combination of a large work function of mercury chalcogenide (HgX) compounds [37] with the narrow band gap nature of the HgX CQDs, bringing the conduction band below the Fermi level of the environment and leading to a degenerate doping in those CQDs [35].

One interesting feature regarding self-doping comes from its tunability. As it has been previously mentioned, doping will depend on the screening of the surface excess cations.

Thus, tuning the surface chemistry of the CQDs, by changing ligands [33,35] or growing a shell [,], is a way to tune its doping. This effect has been evidenced by Robin et al [33], see Fig. 3(a-b). Depending on the capping agent of the CQDs, the ratio of the intraband to interband can be strongly tuned (Fig. 3(a)), which results from the tuning of the 1Se state position (and from its associated population) around the Fermi level. Quantitatively this combination of size [30,33] and surface chemistry [35] can be used to finely tune the doping by more than a decade, with an accuracy better than 0.1 electron per CQD control, see Fig. 3(b). Using a combination of IR spectroscopy, photoemission measurements and numerical simulation, Martinez *et al* [33] have obtained a phase diagram relating the doping level of the CQD (i.e. the position of the Fermi level) as a function of the confinement energy, see Fig. 3(c). For large enough particles, HgSe CQD are systematically degenerately doped (i.e. the Fermi level is in the conduction band). It also appears that for large nanoparticles, the doping can be strong (>18 electrons per nanoparticle) and several quantum states get filled (1Se, 1Pe and 1De).

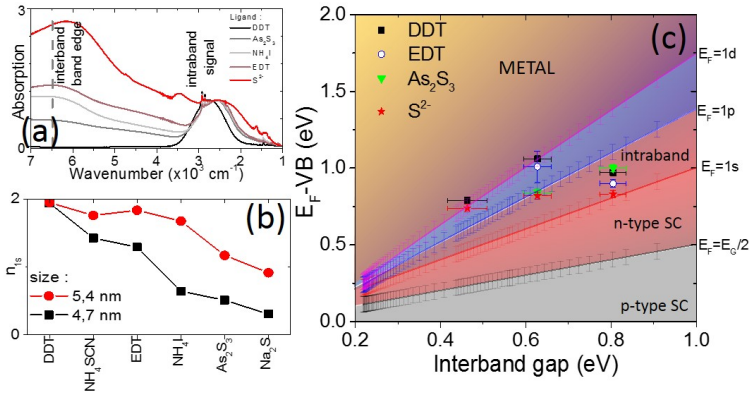

Fig. 3. (a) Absorption spectra of HgSe CQD films with different surface chemistries, adapted with permission from [35], Copyright (2016) American Chemical Society. (b) Change of the population of the conduction band 1S state, as the surface chemistry is tuned, adapted with permission from [35], Copyright (2016) American Chemical Society. (c) Phase diagram of the HgSe CQDs, plotting the relative position of the Fermi energy with respect to the valence band as a function of the confinement energy, for different sizes of HgSe CQDs and different surface chemistries, adapted with permission from [33], Copyright (2017) American Chemical Society.

5. Transport and photodetection properties

The doping is expected to significantly impact the optical and transport properties of the nanoparticle. Actually the mid-IR absorption feature is strictly an intraband transition if the Fermi level is between the 1S and 1P state. If a higher excited state gets filled, the transition continuously acquires a plasmonic character [40] as expected for a (semi) metal with less and less confinement. For III-V semiconductor and nanocrystals, it has been observed that the switch from interband to intersubband/intraband transition come with a reduction of photocarrier lifetime, typically from ns to ps [41,42]. Even shorter lifetime (tens of fs) are expected for plasmon. In this sense the increase of doping is not favorable to photodetection. This decay might nonetheless be partly balanced by an increase of the absorbance per nanoparticle. To date it is not clear rather this emerging intraband/plasmonic colloidal materials have reached a mature level and get limited by fundamental process, however we would like to discuss the currently reported results.

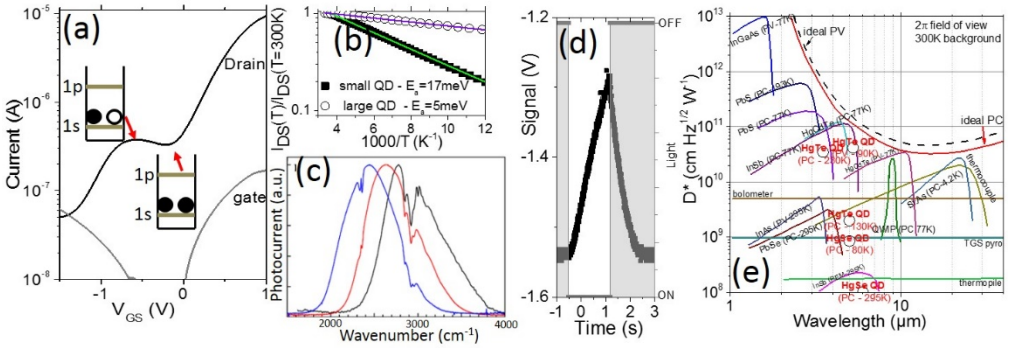

Fig. 4. (a) Transfer curve (drain current vs gate voltage) for a electrolytic field effect transistor, whose channel is made of HgSe CQDs. (b) Current as a function of temperature for thin films of HgSe CQDs with small and large size, adapted with permission from [35], Copyright (2016) American Chemical Society. (c) Intraband photocurrent spectrum form HgSe CQDs films with different sizes, adapted with permission from [24], Copyright (2014) American Chemical Society. (d) Temporal evolution of the photosignal obtained from an HgSe CQDs film under illumination by a 1.55 μm laser diode, adapted with permission from [35], Copyright (2014) American Chemical Society. (e) Map of detectivity as a function of the detector wavelength for different technologies of infrared photodetector, adaptated from [48]. The round dark spot with red text are based on CQDs films.

Transport properties of the self-doped nanocrystals have been investigated in a phototransistor configuration, where gate effect is obtained using an ion gel electrolyte [43,44]. The transfer curve (drain current vs gate voltage) confirms the n–type character of the HgSe CQDs [25,45], see Fig. 4(a). Even more interestingly, the non-monotonic behavior of this curve is the signature of the Pauli blockade, the transconductance of the film reaches a maximum while the CQDs get filled with 1 electron per nanoparticle and then decreases until the 1S state is fulfilled. [46] So far intraband CQD-based materials (see Fig. 4 (c)) have been suffering from two main drawbacks regarding their use for photodetection. The temperature dependence of the current is weak: activation energy extracted from an Arrhenius fit of the conductance (see Fig. 4 (b)) is much smaller (few meV or few tens of meV depending on CQD size) than the optical band gap. In other words, cooling barely improves the signal to noise ratio for photoconduction. Moreover, the time response is slow (several seconds), see Fig. 4 (d). These two limitations will have to be addressed to make intraband CQDs an effective material for photodetection. In terms of photodetection performance, HgSe materials present a high photoresponse, which can be as high as several 100 mA.W-1 for MWIR detection wavelength under low bias operation (1 V typically). Boost of the photoresponse by using plasmon resonance has also been demonstrated [47]. On the other hand, HgSe CQD films suffer from a pretty high dark current, which is, as it was for QWIP technology, inherent to their high doping. This makes that the overall detectivity of HgSe intraband photodetectors is one order of magnitude lower than the one currently obtained from HgTe interband CQDs [48], see Fig. 4 (e).

6. Alternative materials

To finish our discussion, we would like to mention current possible alternatives to mercury chalcogenides, which also present some mid-IR intraband/plasmonic character. Silver chalcogenides have mostly been studied because of their thermoelectric properties. The Norris' group [49,50] also investigate their IR absorption and observe that Ag_2Se present a very similar spectrum to the one of HgSe, see Fig. 5 (a). Even though, the exact nature (intraband vs plasmonic) of this mid-IR transition still need to be clarified. Doped oxides [51] such as Al or Ga [52] doped ZnO [53–55], SnO_2 [56] or In_2O_3 [57–59] constitute another class of mid IR active material, see Fig. 5(b). Beyond the material challenge and the low

toxicity, the main application that has driven the interest for doped oxides is their electrochromic properties [53], with in mind the design of smart windows. Finally, doped silicon nanoparticles have also been reported as mid IR active material [60-62]. In this case the appearing of a plasmonic feature in the mid IR, requires quite a high doping (several tens of %), which is probably closer to an alloying than conventional doping. The obtained feature is quite broad ($\Delta\lambda/\lambda$>100%), see Fig. 5(c). As explained by Delerue [51], the broad plasmonic feature is the result of the strong Coulombic scattering due to the spatial overlap of the free electrons with the ionized impurities. Transport has been investigated in arrays of doped Si nanoparticles to observe the metal insulator transition as the doping level is tuned [60].

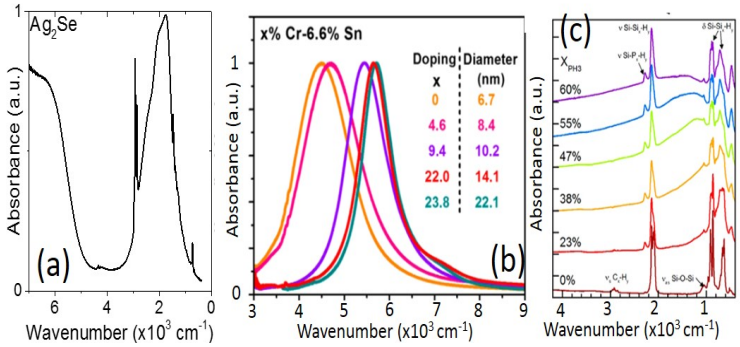

Fig. 5. (a) Infrared absorption spectrum of Ag2Se CQDs. (b) Absorption spectrum of Cr-Sn Doped In_2O_3 CQDs, adapted with permission from [59], Copyright (2014) American Chemical Society. (c) Absorption spectrum of P doped Si nanocrystals, adapted with permission from [63], Copyright (2014) American Chemical Society.

7. Conclusion and perspectives

Thanks to strong chemical progresses, stable intraband and plasmonic transitions can now be reliably obtained from the near-IR up to the THz range of wavelengths. Such transitions have been obtained either by the introduction of extrinsic dopant impurities in oxides and silicon nanoparticles or result from self-doping due to the non-stoichiometry of the synthesized nanoparticles. While many materials can address this range of wavelengths, only the mercury-based materials have so far led to photoconductive properties and raised the hope for the design of a new generation of low cost detectors. Currently, intraband devices still suffer from three main limitations, which are a large dark current, a small thermal activation energy and a slow photoresponse. All these points will have to be addressed to make intraband transition-based devices match the performance of interband transition-based ones. Intraband colloidal materials remain nevertheless of utmost interest because of new possibilities for longer wavelength availability, device geometries and we can hope for the emergence of structures as complex as quantum cascade devices only based on colloidal materials.

Funding

ERC (756225); Region Ile-de-France; ANR (ANR-11-IDEX-0004-02, MATISSE, H2DH).

Acknowledgments

EL thanks the support of ERC starting grant (project: blackQD - grant 756225). This work has been supported by the Region Ile-de-France in the framework of DIM Nano-K via the grant dopQD. This work was supported by French state funds managed by the ANR within the Investissements d'Avenir program under reference ANR-11-IDEX-0004-02, and more specifically within the framework of the Cluster of Excellence MATISSE and grant H2DH.